Counter-Rotating Gyres as a Non-Local Effect of Resonating Basin Modes

Baylor Fox-Kemper

NOAA Climate and Global Change Program and Princeton University Atmospheric and Oceanic Sciences Program

P.O. Box 308, Princeton, NJ 08542, baylor@princeton.edu

OS21F-12

I. Abstract

Relatively high Reynolds number calculations of a barotropic ocean model reveal counter-rotating gyres on the eastern side of the basin. These unintuitive regions rotate in a direction opposite to the wind forcing direction, and are sometimes associated with strong up-gradient vorticity fluxes. An analysis of the empirical orthogonal functions of some numerical calculations reveals that much of the variance is in oscillations resembling basin modes. A simple non-local model of the nonlinear interaction of forced-dissipative basin modes, together with the observed variance of each mode in the numerical calculation, gives excellent agreement with the streamfunction and dynamical balances of the counter-rotating gyres.

(Fox-Kemper, 2003)

II. Model

The model results presented here are from a 257x257 Chebyshev polynomial pseudo-spectral numerical barotropic model in a rectangular basin with spatially-variable viscosity to roughly parameterize boundary physics not directly represented in the model. The nondimensional equations governing the model are:

$$\frac{\partial\zeta}{\partial t} + \nabla\cdot(\hat{\mathbf{x}}\psi + \delta_I^2\mathbf{u}\zeta - \delta_M^3\nabla\zeta + \delta_S\nabla\psi) = -\sin(\pi y), \quad (1)$$

$$\zeta = \nabla^2\psi, \quad (2)$$

$$\delta_M^3 = \frac{\delta_I^3}{\mathrm{Re_i}} + \left(\frac{\delta_I^3}{\mathrm{Re_b}} - \frac{\delta_I^3}{\mathrm{Re_i}}\right)\left(e^{-x/\delta_d} + e^{-(1-x)/\delta_d}\right), \quad (3)$$

$$\delta_d \equiv \frac{\delta_I}{\sqrt{\mathrm{Re_i}}}, \quad (4)$$

where ψ (streamfunction) and ζ (relative vorticity) are determined during integration. Boundary conditions are slip (ζ=0) on the 'fluid' boundaries and no-slip ($\frac{\partial\psi}{\partial x}=0$) on the 'solid' boundaries, as well as impermeability on all boundaries ($\psi=0$). The basin domain is y between 0 and 1 and x between 0 and x_e. The other parameters are δ_I (Charney, 1955, inertial boundary layer width), δ_S (Stommel, 1948, frictional boundary layer width), and $\mathrm{Re_i}$ and $\mathrm{Re_b}$ are Reynolds numbers for the interior and boundary viscosity (Munk, 1950). Throughout, δ_I is 0.02 and δ_S is 0, while $\mathrm{Re_i}$ and $\mathrm{Re_b}$ vary.

III. Results

III.a. Counter-Rotating Gyres

The enhanced viscosity near the boundary allows for much higher interior Reynolds number without inertial domination (Fox-Kemper and Pedlosky, 2003).

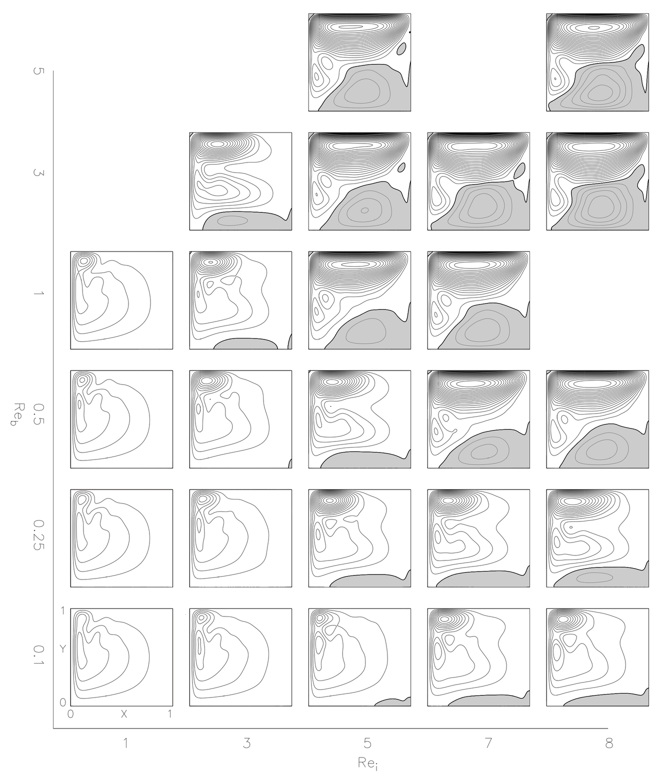

The time-mean streamfunction for a number of parameter settings shows regions rotating counter to the wind stress.

III.b. Resonating Basin Modes

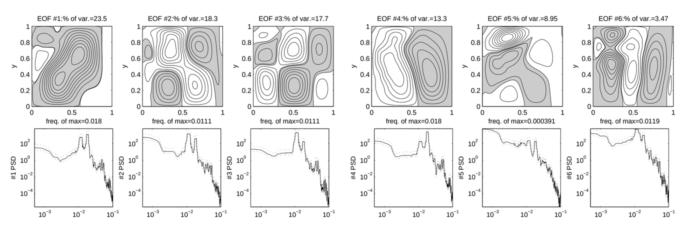

The ψ EOFs and PSDs of EOF presence for a $\mathrm{Re_b}$=0.25, $\mathrm{Re_i}$=5 calculation.

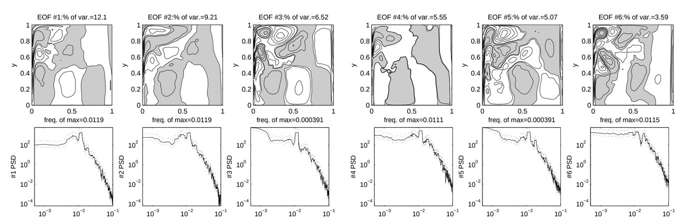

The ζ EOFs and PSDs of EOF presence for a $\mathrm{Re_b}$=0.25, $\mathrm{Re_i}$=5 calculation.

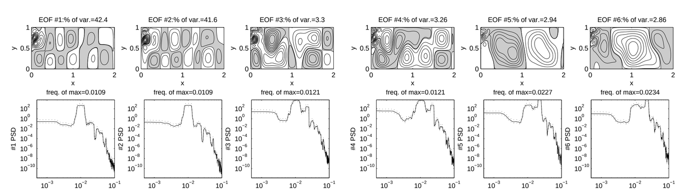

The ψ EOFs and PSDs of EOF presence for a $\mathrm{Re_b}$=1, $\mathrm{Re_i}$=1 calculation in an elongated basin.

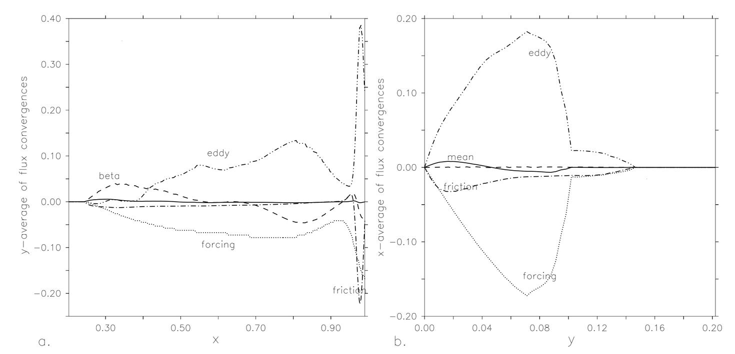

(a) and (b) show the meridional and zonal averages, respectively, of vorticity flux convergences in the region where $\overline{\psi} < 0$ (the counter-rotating gyre) from the $\mathrm{Re_b}$=0.25, $\mathrm{Re_i}$=5 calculation.

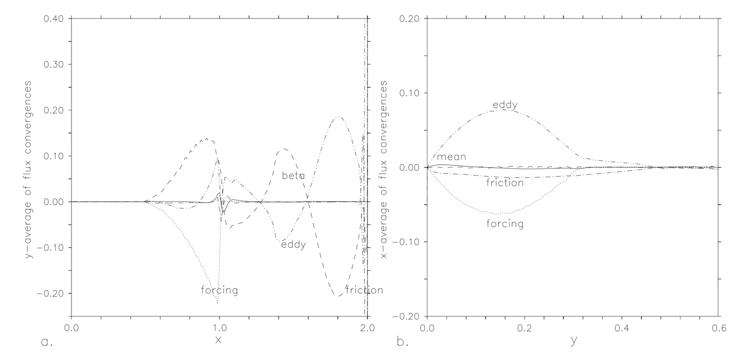

(a) and (b) show the meridional and zonal averages, respectively, of terms in (5) in the region where $\overline{\psi} < 0$ (the counter-rotating gyre) from the $\mathrm{Re_i}$=$\mathrm{Re_b}$=3 elongated basin calculation with wind only in the western half of the basin.

Counter-rotating gyres in other models have been attributed to Fofonoff (1954) gyres (predicted by inviscid statistical mechanics Griffa and Castellari, 1991; Özgökmen and Chassignet, 1998), mixing of absolute vorticity (Greatbatch and Nadiga, 1999), and nonlinear dispersion (Holm and Nadiga, 2003). However, the Fofonoff (1954) primary is mean vorticity advection and β-term; some regions would require 'up-gradient' absolute vorticity fluxes; and the gyres have a sensitive dependence on the frequency of the boundary current instabilities not captured by the dispersion model.

In summary,

- EOFs strongly resemble spatial structure of basin mode standing waves with two EOFs per basin mode.
- PSDs of EOF presence have peaks at basin mode frequencies.
- Vorticity EOFs reveal that most variance in in boundary current region, but frequency matches that of the resonating modes.
- Thus, there are basin modes forced by boundary current instabilities.
- The counter-rotating gyres occur on the eastern side, where basin modes are the most important variability, and their vorticity balance depends critically on eddy flux divergences.

IV. Theory

Consider a grossly simplified model, replacing Laplacian friction with bottom drag and representing the boundary mode instabilities as an additional forcing.

$$\frac{\partial\nabla^2\psi}{\partial t} + \frac{\partial\psi}{\partial x} + \delta_I^2 J(\psi,\nabla^2\psi) + \delta_S\nabla^2\psi = -\sin(\pi y) + A_f\sin(n_f\pi y)\cos(\omega_f t)e^{-x/\delta_f}. \quad (5)$$

Consider the weakly nonlinear perturbation series: $\psi = \psi_0 + \epsilon\psi_1 + \ldots$ under the assumption that $\delta_I \ll 1$. The ψ_0 equation is linear, so it is uncoupled into a steady equation (similar to Stommel (1948)) and a time-dependent equation (similar to Pedlosky, 1965). By differentiating the linear solutions, the first nonlinear correction can be calculated. If the periodic forcing is resonant with a basin mode, then the results are to lowest order in δ_S:

$$\delta_I^2 J(\overline{\psi_0},\nabla^2\overline{\psi_0}) \approx \tfrac{1}{2}\pi^3\delta_S\delta_I^2\sin(2\pi y), \quad (6)$$

$$\delta_I^2\overline{J(\psi_0',\nabla^2\psi_0')} \approx \frac{2m^3 n_f\pi^4\omega_f^4|\varphi_0|^2\delta_I^2}{\delta_S^2}\sin(2m\pi x)\sin(2n_f\pi y)\left(1 - 2(-1)^m e^{-\frac{1}{\delta_f}}\cos\left(\frac{1}{2\omega_f}\right) + e^{-\frac{2}{\delta_f}}\right).$$

The resulting mean vorticity flux convergence is very large within the western boundary current but $O(\delta_S\delta_I^2)$ outside it. On the other hand, the eddy term is $O(|\varphi_0|^2\delta_I^2/\delta_S^2)$ outside of the forcing region. The analytic eddy flux divergence gives approximate nonlinear interaction outside of the boundary current region, resulting in a correction to Sverdrup flow.

$$\overline{\psi_0} + \overline{\psi_1} = (1-x)\sin(\pi y) + \int_1^x \delta_I^2\overline{J(\psi_0',\nabla^2\psi_0')}\mathrm{d}x. \quad (7)$$

Although the strength of each basin mode depends in a complicated way on the boundary current instabilities, the eddy interaction as a function of the average variance of the basin mode, which we can deduce from the EOFs.

$$\delta_I^2\overline{J(\psi_0',\nabla^2\psi_0')} \approx 4\pi^4 m n_f(m^2+n_f^2)\delta_I^2\sin(2m\pi x)\sin(2n_f\pi y)\int_0^1\int_0^1\overline{(\psi_0')^2}\mathrm{d}x\mathrm{d}y, \quad (8)$$

V. Confirmation of Theory

The variances of a few basin modes are deduced from the EOFs of a model calculation. The nonlinear interaction of the *analytic* basin modes produces good agreement with the interior solution, including the counter-rotating regions.

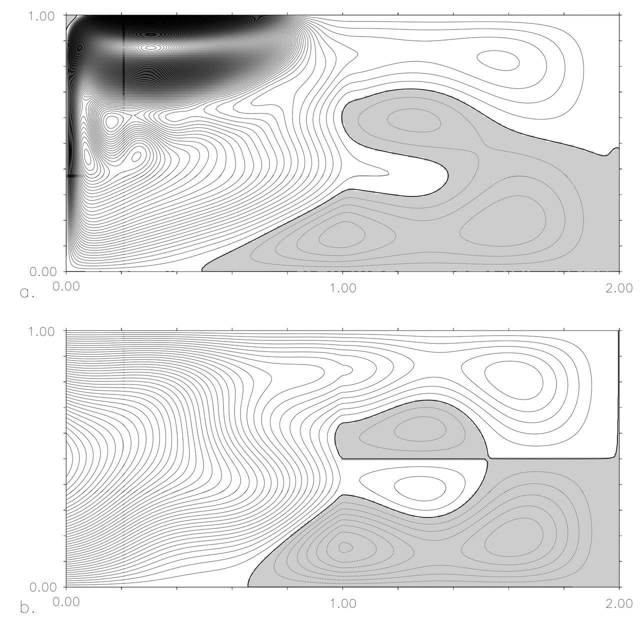

a) The time-mean streamfunction in a elongated basin with $\mathrm{Re_b}$=3, $\mathrm{Re_i}$=3. There is wind forcing only in the western half of the basin. b) The prediction with analytic basin modes (3,1), (2,1), (1,2), (1,1), and (2,2) with variances from EOF diagnosis.

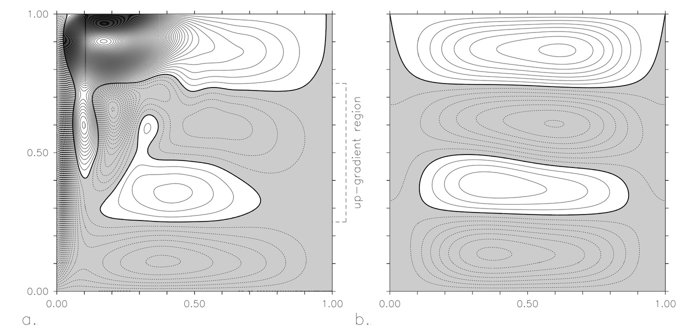

a) The time-mean streamfunction minus the Sverdrup (1947) interior solution for the $\mathrm{Re_b}$= 0.25, $\mathrm{Re_i}$= 5 calculation reveals a counter-rotating and co-rotating gyre pattern irreconcilable with a local down-gradient absolute vorticity flux. b) The prediction using basin modes (1,1), (1,2), (2,1), and (2,2) with variances from EOF diagnosis.

VI. Conclusions

- *Basin modes dominate the variability of the basin interior.*
- *These basin modes resonate and are forced by instabilities of the western boundary current.*
- *In the basin interior, basin modes, not vortices or mean-mean interaction dominates the nonlinearity.*
- *Calculating the nonlinear interaction of analytic basin modes with the variances from EOFs gives good agreement for deviations from Sverdrup (1947) interior flow.*

References

Charney, J. G.: 1955, The gulf stream as an inertial boundary layer. *Proceedings of the National Academy of Sciences*, **41**, 731–740.

Fofonoff, N. P.: 1954, Steady flow in a frictionless homogenous ocean. *Journal of Marine Research*, **13**, 254–262.

Fox-Kemper, B.: 2003, Wind-driven barotropic gyre II: Effects of eddies and low interior viscosity. *submitted to the Journal of Marine Research*.

Fox-Kemper, B. and J. Pedlosky: 2003, Wind-driven barotropic gyre I: Circulation control by eddy vorticity fluxes to a region of enhanced removal. *submitted to the Journal of Marine Research*.

Greatbatch, R. J. and B. T. Nadiga: 1999, Four-gyre circulation in a barotropic model with double-gyre wind forcing. *Journal of Physical Oceanography*, **30**, 1461–1471.

Griffa, A. and S. Castellari: 1991, Nonlinear general circulation of an ocean model driven by wind with a stochastic component. *Journal of Marine Research*, **49**, 53–73.

Holm, D. D. and B. T. Nadiga: 2003, Modeling mesoscale turbulence in the barotropic double gyre circulation. *Journal of Physical Oceanography*, **33**, 2355–2365.

Munk, W. H.: 1950, On the wind-driven ocean circulation. *Journal of Meteorology*, **7**, 79–93.

Özgökmen, T. and E. P. Chassignet: 1998, Emergence of inertial gyres in a two-layer quasigeostrophic ocean model. *Journal of Physical Oceanography*, **28**, 461–484.

Pedlosky, J.: 1965, A study of the time dependent ocean circulation. *Journal of the Atmospheric Sciences*, **22**, 267–272.

Stommel, H. M.: 1948, The westward intensification of wind-driven ocean currents. *Transactions, American Geophysical Union*, **29**, 202–206.

Sverdrup, H. U.: 1947, Wind-driven currents in a baroclinic ocean; with application to the equatorial currents of the eastern Pacific. *Proceedings of the National Academy of Sciences*, **33**, 318–326.